한국복합신소재구조학회 논문집 제4권, 제1호, 2013년 03월
J. Korean Soc. Adv. Comp. Struc. Vol. 4, No. 1, pp. 25-32, March 2013
DOI http://dx.doi.org/10.11004/kosacs.2013.4.1.025

ISSN 2093-5145(Print)
ISSN 2288-0232(Online)

주기하중을 받고 있는 금속의 시간의존적 소성 모델 비교

김동건[1] · Gary Dargush[2]

한국수력원자력 중앙연구원 선임연구원[1]
The State University of New York at Buffalo, Department of Mechanical & Aerospace Engineering, Professor[2]

A Rate Dependent Plasticity Model under Cyclic Loading of Metals

Dongkeon Kim[1] · Gary F. Dargush[2]

[1]Senior Researcher, Central Research Institute, Korea Hydro & Nuclear Power Co., LTD, Daejeon 305-343, Republic of Korea
[2]Professor, Department of Mechanical and Aerospace Engineering, University at Buffalo, The State University of New York, Buffalo, NY 14260, USA

Abstract: In real world applications, the response of structures may be dependent on the rate of loading and thus can be affected by transient loading, especially when the rate of loading is significant. In such situations, the rate of loading may become a major issue to understand structures during earthquake excitation or under blast or high velocity impact. In some cases, the rate effect on structures under strong earthquake excitation cannot be ignored when attempting to understand inelastic behavior of structures. Many researchers developed the constitutive theories in cyclic plasticity and viscoplasticity. In this study, numerical simulation by cyclic visocoplasticity models is introduced and analyzed. Finally, the analytical results are compared with experimental results as a means to evaluate and verify the model.

Key Words: Rate dependent, viscoplasticity, cyclic plasticity, Constitutive model

1. Introduction

The plasticity of materials which undergo irreversible deformations and exhibit rate effects is called as viscoplasticity. Thus, it is defined as rate dependent plasticity or time dependent plasticity in which crystallographic slip is dominant during deformation processes. These models are appropriate and often required to analyze properly the behavior of materials subjected to transient loading. Also, viscoplasticity can be applied to creep, which is described as low strain rate, time dependent irreversible deformation for long term response, whether the process is controlled by diffusion or affected by diffusion.

Viscoplasticty is referred to the mechanical response of solids involving time dependent, irreversible strains (Lemaitre, 2001). For viscoplasticity, elastic strain and the strain hardening rule are the same as those in plasticity. Rate independent plasticity models mentioned in the previous section, cannot describe time dependent inelastic behavior of material, such as strain rate effect, stress rate for ratchetting, and hold time. Thus, these viscoplasticity models have been developed to consider the character of rate dependence and to establish correlation with experimental results.

Bodner and Partom (1972) started to establish a viscoplastic theory. Their unified theory described an approach that inelastic behavior of plasticity and viscoplasticity was not separated. Miller, (1976), Robinson et al. (1976), Hart (1976), Krempl (1979) studied this theory, and Chaboche (1977) developed a

주요어: 유한요소해석, 최대매설깊이, 최소매설깊이, 플래스틱

Corresponding author: Kim, Dongkeon
Central Research Institute, Korea Hydro & Nuclear Power Co., LTD, Daejeon 305-343, Republic of Korea
Tel: +82-31-400-4685, Fax: +82-31-406-7118, E-mail:dkkzone@gmail.com

투고일: 2013년 2월 4일 / 수정일: 2013년 2월 19일 / 게재확정일: 2013년 3월 8일

viscoplastic constitutive model with nonlinear kinematic hardening, and Chaboche and Rousselier (1983) applied this model to the 316 stainless steel. Ellyin and Zia (1991) then used this viscoplasticity model for stainless steel 304 and 316. McDowell (1992) developed viscoplastic nonlinear kinematic hardening model under thermomechanical cyclic conditions, while Tanaka (1994) developed a viscoplastic constitutive model under nonproportional loading.

Chaboche and Rousselier (1983) used their viscoplasticiy model for the simulation of ratchetting. Ohno and Wang (1993) combined a modified Armstrong-Frederick model and viscoplastic equation. Tanaka and Yamada (1993), and Abdel-Karim and Ohno (2000) continued with this study. This rate-dependence of ratchetting has been done by Kang and Gao (2004), Yaguchi and Takahashi (2000), Yaguchi and Takahashi (2005), and Kang et al. (2006).

For rate independent models, the stress-strain response is assumed to be independent of the rate of loading, whether loading is strain-controlled or stress-controlled. The rate of loading may become a major issue to understand structures during earthquake excitation or under blast or high velocity impact. In some cases, the rate effect on structures under strong earthquake excitation cannot be ignored when attempting to understand inelastic behavior of structures. In this study, numerical simulation by cyclic visocoplasticity models is introduced and analyzed. Finally, the analytical results by ABAQUS (Hibbit, Karlsson and Sorensen, 2008) are compared with experimental results as a means to evaluate and verify the model.

2. Constitutive model

In plasticity, consistency conditions are used to enforce the load point to stay on the yield stress during plastic deformation. In contrast to this, the load point may lie outside the yield surface because of its viscosity and overstress in viscoplasticity. The total strain at a given stress can be decomposed into three parts (elastic, viscoplastic, and thermal components) for the classical viscoplastic approach or four parts (adding a plastic strain rate) for combined rate independent and rate dependent response. Thus, for these two cases, one may write

$$\dot{\varepsilon}_{ij} = \dot{\varepsilon}_{ij}^{e} + \dot{\varepsilon}_{ij}^{vp} + \dot{\varepsilon}_{ij}^{T} \tag{1}$$

$$\dot{\varepsilon}_{ij} = \dot{\varepsilon}_{ij}^{e} + \dot{\varepsilon}_{ij}^{p} + \dot{\varepsilon}_{ij}^{vp} + \dot{\varepsilon}_{ij}^{T} = \dot{\varepsilon}_{ij}^{e} + \dot{\varepsilon}_{ij}^{In} + \dot{\varepsilon}_{ij}^{T} \tag{2}$$

Since viscoplastic and plastic strains are not independent, the term inelastic strain is mostly used. The elastic strain is given by the stress tensor with usual linear elastic equations. That is,

$$\dot{\sigma}_{ij} = C_{ijkl}^{e} \dot{\varepsilon}_{kl}^{e} \tag{3}$$

and, thus, the elasto-inelastic relation is written as

$$\dot{\sigma}_{ij} = C_{ijkl}^{e} (\dot{\varepsilon}_{kl} - \dot{\varepsilon}_{kl}^{In}) \tag{4}$$

where C^e is the elastic constitutive matrix, $\dot{\varepsilon}^e$ is the elastic strain increment, $\dot{\varepsilon}^{vp}$ is the viscoplastic strain increment, $\dot{\varepsilon}^p$ is the plastic strain increment, $\dot{\varepsilon}^T$ is the thermal strain increment, and $\dot{\varepsilon}^{In}$ is the inelastic strain increment. The viscoplastic strain rate is computed from the normality hypothesis

$$\dot{\varepsilon}_{ij}^{vp} = \dot{p} \frac{\partial g}{\partial \sigma} \tag{5}$$

where g is the flow potential, which in general is function of stress, temperature and state variables. Based on a von Mises yield surface, as is used in rate independent plasticity, the effective stress, and effective strain rate become

$$\sigma_e = \sqrt{\frac{2}{3} S_{ij} S_{ij}} \tag{6}$$

and

$$\varepsilon_e = \sqrt{\frac{2}{3} \varepsilon_{ij} \varepsilon_{ij}} \tag{7}$$

respectively. Thus, the viscoplastic plastic strain rate is written as

$$\dot{\varepsilon}_{ij}^{vp} = \frac{3}{2} \dot{p} \frac{S_{ij}}{\sigma_e} \tag{8}$$

To consider strain hardening, a stress function is needed to relate the increase in stress with strain. The may be a quite general function of stress. However, usually a power law, exponential or hyperbolic function is postulated. Bodner and Partom (1972) originally used the following exponential type function, which is usually best for slip at high velocity:

$$\dot{\varepsilon}_{ij}^{In} = C\exp\left[-\frac{1}{2}\left(\frac{Z^2}{3\mathrm{J}_2}\right)^n\right]\frac{S_{ij}}{\sqrt{J_2}} \tag{9}$$

where constant C is a scale factor that corresponds to the maximum inelastic strain rate, n is a controlling parameter for strain-rate sensitivity, and Z is a state variable for both the isotropic and kinematic hardening rule. Ramaswamy and Stouffer (1990) modified the Bodner equation to include back stress, as in

$$\dot{\varepsilon}_{ij}^{In} = C\exp\left[-\frac{1}{2}\left(\frac{Z^2}{3\mathrm{T}^2\mathrm{K}_2}\right)^n\right]\frac{S_{ij}-X_{ij}}{\sqrt{K_2}} \tag{10}$$

where T is absolute temperature, and K_2 is the norm of the difference between the stress and back stress. Meanwhile, Miller(1976) proposed a sine hyperbolic type function introducing back stress and drag stress as follows:

$$\dot{\varepsilon}_{ij}^{In} = \frac{3}{2}C\left[\sinh\left(\frac{\sqrt{K_2}}{\mathrm{Z}}\right)^{3/2}\right]^n\frac{S_{ij}-X_{ij}}{\sqrt{K_2}} \tag{11}$$

Chaboche (1989) used a modified power law function, created by adding a second power law to the flow rule to reduce numerical difficulties. The resulting function can be written

$$\dot{\varepsilon}_{ij}^{In} = \frac{3}{2}\left[\left(\frac{\sqrt{3K_2}}{\mathrm{Z}}\right)^{n_1}+\left(\frac{\sqrt{3K_2}}{\mathrm{Z}_2}\right)^{n_2}\right]\frac{S_{ij}-X_{ij}}{\sqrt{3K_2}} \tag{12}$$

In the remainder of this section, some basic background for viscoplasticity will be introduced with isotropic and kinematic hardening rules and comparisons with plasticity. Finally, these viscoplastic definitions and strain hardening rules will be used for the formulation of a rate dependent two surface model.

2.1 Viscoplasticity With Kinematic Hardening Rule

Kinematic hardening rule in viscoplasticity also has the same concept as in plasticity. Thus, the yield surface translates in stress space, rather than expanding. However, now one must consider also the viscous stress. Thus, the kinematic hardening rule in viscoplasticity is followed by same procedures in plasticity and is explained below.

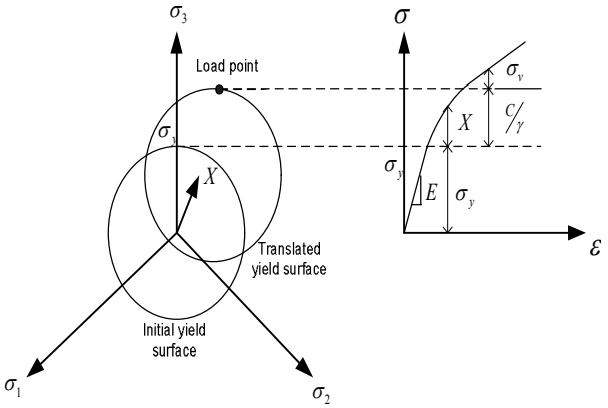

Fig. 1 Von mises yield surface for viscoplasticity with linear kinematic hardening in stress space and stress-strain curve (Dunne and Petrinic, 2005)

As shown in Fig. 1, the von Mises yield surface is translated from the initial yield surface by a linear kinematic hardening rule. The resulting stress-strain to explain the form of viscoplasticity is shown in right figure. The increment in back stress for linear kinematic hardening and nonlinear kinematic hardening are given, respectively, by

$$\dot{x} = \frac{2}{3}c\dot{\varepsilon}^p \tag{13}$$

$$\dot{x} = \frac{2}{3}c\dot{\varepsilon}^p - \gamma x\dot{p} \tag{14}$$

where c and γ are material constants. For rate independent plasticity, the stress is given by combining the yield stress (σ_y) and the contribution by linear kinematic hardening
(c / γ). Thus,

$$\sigma = \sigma_y + c/\gamma \tag{15}$$

However, for rate dependent plasticity, the stress is calculated by adding the viscous stress to the above equation. This viscous stress is used as a power law function.

Consequently, the stress is given by

$$\sigma=\sigma_y+c/\gamma+\sigma_v=\sigma_y+c/\gamma+Y\dot{p}^m \tag{16}$$

By rearranging Eq. (16), the effective strain is given by

$$\dot{p}=\left(\frac{\sigma-x-\sigma_y}{Y}\right)^{\frac{1}{m}} \tag{17}$$

The above equation is the constitutive relation between effective plastic strain rate and stress for the uniaxial case, involving some internal variables. For multi-axial cases, the effective strain rate is written by

$$\dot{p}=\left(\frac{J(S-X)-\sigma_y}{Y}\right)^{\frac{1}{m}} \tag{18}$$

The yield function is given by

$$g=J(S-X)-\sigma_y \tag{19}$$

and with the normality rule, the components of the plastic strain rate are written by

$$\dot{\varepsilon}_{ij}^{vp}=\dot{p}\frac{\partial g}{\partial\sigma}=\frac{3}{2}\dot{p}\frac{S-X}{J(S-X)} \tag{20}$$

Finally, the viscoplastic stress-strain relation is obtained through Hooke's law by

$$\dot{\sigma}_{ij}=C_{ijkl}^e(\dot{\varepsilon}_{kl}-\dot{\varepsilon}_{kl}^{vp})=C_{ijkl}^e\left(\dot{\varepsilon}_{kl}-\frac{3}{2}\dot{p}\frac{S-X}{J(S-X)}\right) \tag{21}$$

Thus, this viscoplastic stress-strain equation with kinematic hardening rule shows that stresses are determined at the end of the given step forward in time with current total strain increment, kinematic hardening variables, yield stress and a given time.

3. Numerical results for A36 steel subjected to monotonic loading

Chang and Lee (1987) tested A36 structural steel under monotonic loading to understand the strain rate effect. The monotonic loading with the rate of 10^{-3}/sec, 10^{-4}/sec, and 10^{-5}/sec was increased until 2% axial strain was achieved. Three stress levels corresponding to the given strain rates were observed, respectively, 32.5 ksi, 30 ksi, and 28.5 ksi, as shown in Fig.2. Thus, some strain rate sensitivity was observed, which indicates that the faster strain rate gives higher yield stress. Also, the higher strain rates gave the longer plastic plateau. With reference to a strain rate of 10^{-5}/sec, the yield stress at a strain rate of 10^{-4}/sec was increased by 5%, and the yield stress at strain rate of 10^{-3}/sec was increased by 14%. These experimental results are compared with the rate dependent kinematic hardening and two surface models in the next sections.

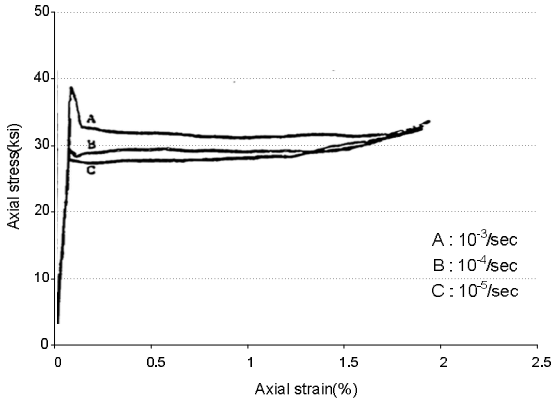

Fig. 2 Monotonic loading stress-strain response depending on three different rates of three identical specimens (Chang and Lee, 1987)

3.1 Numerical Result by Rate Ddependent Kinematic Hardening Model

The rate dependent kinematic hardening model is implemented as a user subroutine in the finite element software ABAQUS. A simplified model of the original cylinder-type specimen is modeled in ABAQUS, using four node bilinear axisymmetric elements (CAX4). Numerical results for steel under monotonic loading by the rate dependent kinematic hardening model is shown in Fig. 3. Material properties and material parameters for the kinematic hardening model are shown in Table 1. Material parameters are determined by adjustment to

achieve the best analysis results. The initial axial yield stress is 30 ksi, but a value of 26.1 ksi is used as the yield stress for this model, because there are viscous stresses outside the yield surface. The three stress levels at the given strain rates were simulated as 32.3 ksi, 30ksi, and 28.6 ksi, respectively. Analytical results do show strain rate sensitivity, indicating that the faster strain rate gives higher yield stress. Thus, numerical result by rate dependent kinematic hardening model gives reasonably good results for analysis of steel under monotonic loading.

Table 1. Material properties and rate dependent kinematic hardening model parameters for A36 structural steel

Young's modulus(E):28,500 ksi (196,500MPa)	Poisson's ratio (υ) : 0.35
Axial initial stress(σ_y) : 30ksi (206.84MPa)	
Material parameters of sine hyperbolic function for kinematic hardening model (C) : 1.E+2	Material parameters of sine hyperbolic function for kinematic hardening model (B) : 1.E-8
Material parameters of sine hyperbolic function for kinematic hardening model (n) : 5.0	Axial initial stress used in model (σ_y):26.1 ksi (180 Mpa)

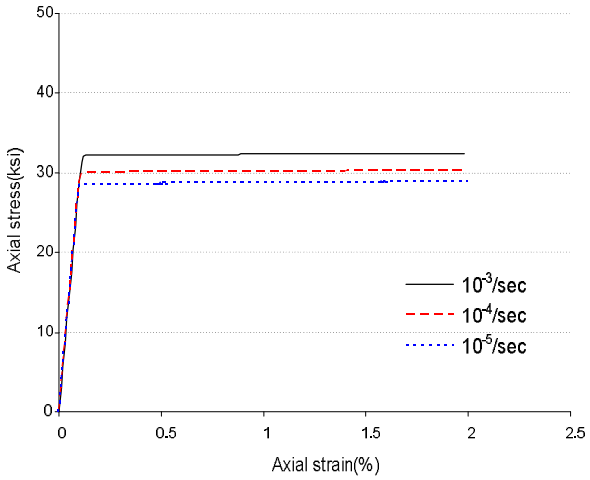

Fig. 3 Monotonic loading stress-strain response depending on three different rates of three identical specimens by rate dependent kinematic hardening model

4. Numerical results of A36 steel subjected to cyclic loading Type 1 and Type 2

Chang and Lee (1987) also tested structural steel under cyclic loading to understand the strain rate sensitivity. The cyclic loading with the rate of 10^{-2}/sec and 10^{-4}/sec was increased until 0.8% axial strain was attained. The loading history is shown in Fig.4 for the strain rate of 10^{-4}/sec and in Fig.5 for the strain rate of 10^{-2}/sec. The specimen was loaded cyclically in the axial direction, with the loading continued until it was stabilized. The stabilized stress-strain curve is shown in Fig.6. There is some strain rate sensitivity observed, which indicates that the faster strain rate gives a higher yield stress. These experimental results are compared with the rate dependent kinematic hardening and two surface models in the next sections.

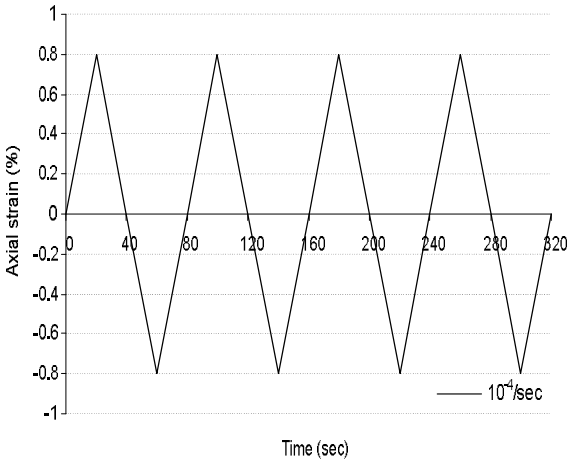

Fig. 4 Cyclic loading history which is used for strain rate of 10^{-4}/sec (LoadingType1)

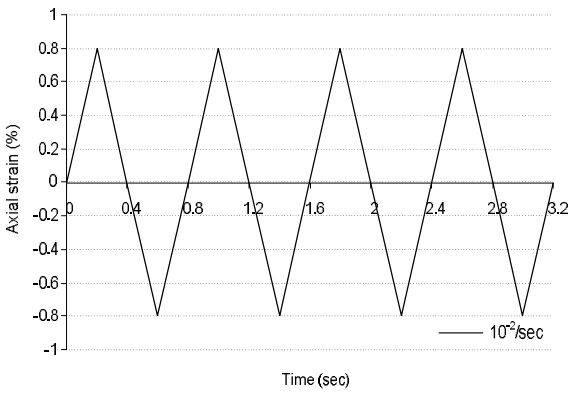

Fig. 5 Cyclic loading history which is used for strain rate of 10^{-2}/sec(LoadingType2)

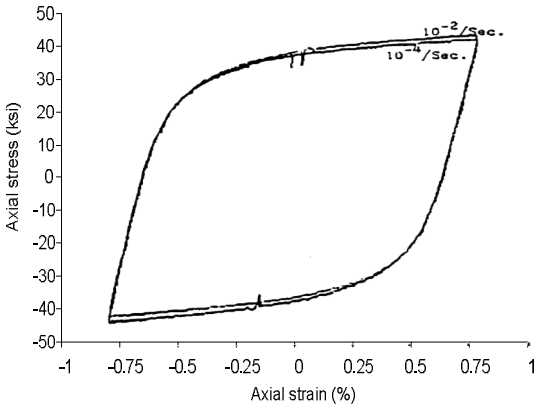

Fig. 6 Stabilized cyclic loading stress-strain response depending on two different rates (10^{-2}/sec and 10^{-4}/sec) (ChangandLee, 1987)

4.1 Numerical Result by Rate Dependent Kinematic Hardening Model

In this analysis, the four node bilinear axisymmetric element (CAX4) is also used for steel under cyclic loading. Numerical results for mild steel under cyclic loading by the rate dependent kinematic hardening model are shown in Fig. 7. Material properties and material parameters for the kinematic hardening model are shown in Table 1. Analytical results also show small strain rate sensitivity, suggesting that the faster strain rate (10^{-2}/sec; solid line) gives higher yield stress than the slower strain rate (10^{-4}/sec; dotted line). The numerical results from the rate dependent kinematic hardening model gives acceptable results in terms of maximum stress, but it does not provide a good shape to the hysteresis loop in the plastic range, after yielding.

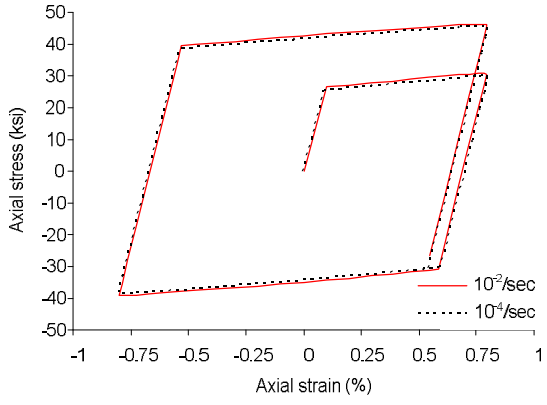

Fig. 7 Cyclic loading stress-strain response depending on two different rates (10^{-2}/sec and 10^{-4}/sec) by rate dependent kinematic hardening model

5. Numerical results of A36 steel subjected to cyclic loading Type 3 and type 4

Chang and Lee (1987) also tested structural steel under Type 3 and Type 4 cyclic loading to understand the strain rate sensitivity. The cyclic loading with the rate of 10-4/sec and 5 x 10-3/sec was applied in ranges 0.6%, 1.2% and 1.5% and the loading history is shown, respectively, in Fig.8 for the strain rate of 10-4/sec and in Fig.9 for the strain rate of 5 x 10-3/sec. Fig.10 shows the result for a strain rate of 10-4/sec and Fig.11 shows the result of a strain rate of 5x10-3/sec. Notice that the stresses for strain rate 5x10-3/sec are higher than the stresses for 10-4/sec (37.5ksi vs. 34ksi at the 0.6% strain, 42.1ksi vs. 39ksi at the 1.2% strain, and 44.7ksi vs. 39ksi at the strain 1.5% strain). These experimental results are compared with the rate dependent kinematic hardening and two surface models the next sections.

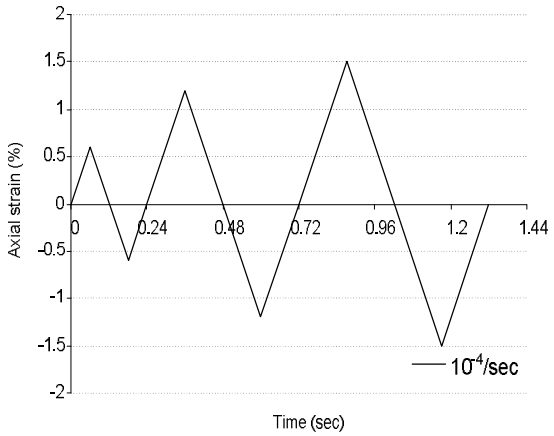

Fig. 8 Cyclic loading history with strain rate of 10^{-4}/sec(Loading Type3)

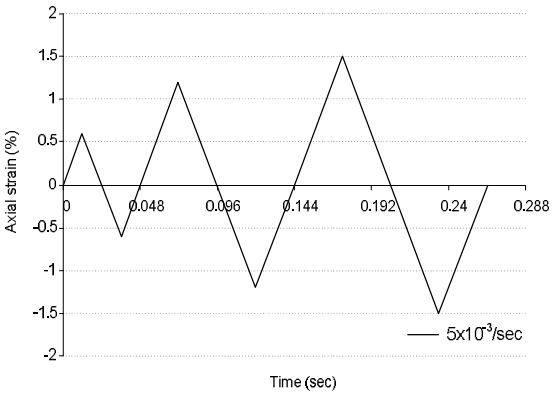

Fig. 9 Cyclic loading history with strain rate of 5 x 10^{-3}/sec(Loading Type4)

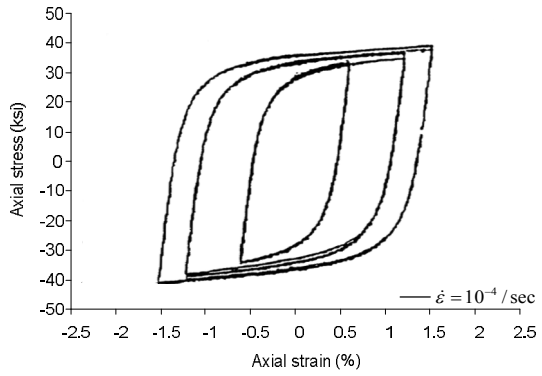

Fig. 10 Cyclic loading stress-strain response with strain rate of 10^{-4}/sec(ChangandLee,1987)

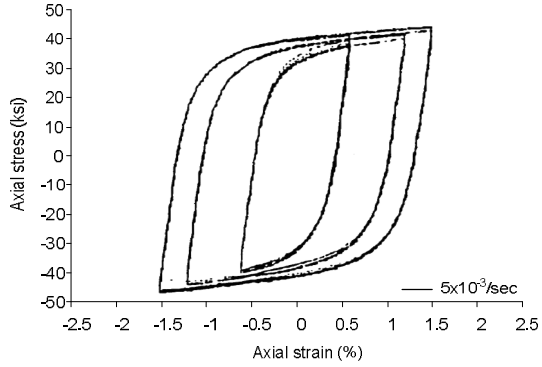

Fig. 11 Cyclic loading stress-strain response with strain rate of 5 x 10^{-3}/sec(ChangandLee,1987)

5.1 Numerical Rresult by Rrate Dependent Kinematic Hardening Model

In the finite element analysis, the four node bilinear axisymmetric elements (CAX4) are again used for steel under Type 3 and Type 4 cyclic loading. Material properties and material parameters for the kinematic hardening model are shown in Table 1. Numerical results for steel under cyclic loading obtained from the rate dependent kinematic hardening model are shown in Fig. 12 and in Fig. 13. The stresses for strain rate 5 x 10^{-3}/sec are higher than stresses for 10^{-4}/sec (36.9ksi vs. 35.3ksi at 0.6% strain, 41.1ksi vs. 39.5ksi at 1.2% strain, and 46.8ksi vs. 45.3ksi at 1.5% strain). Thus, the numerical results from the rate dependent kinematic hardening model are close in terms of the maximum stress at each cycle compared with the experimental data on strain rate effects, but the model gives a linear shape to the stress-strain response in the plastic range after yielding.

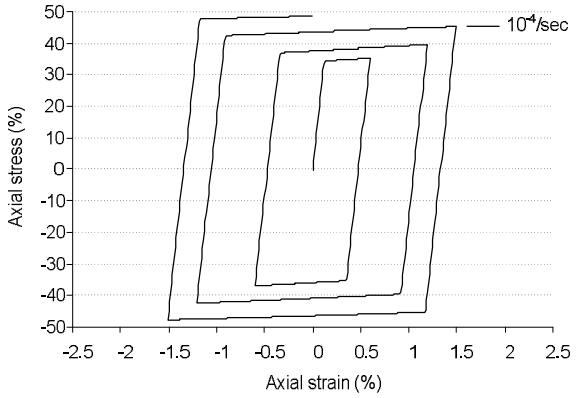

Fig. 12 Cyclic loading stress-strain response for strain rate of 10^{-4}/sec by rate dependent kinematic hardening model

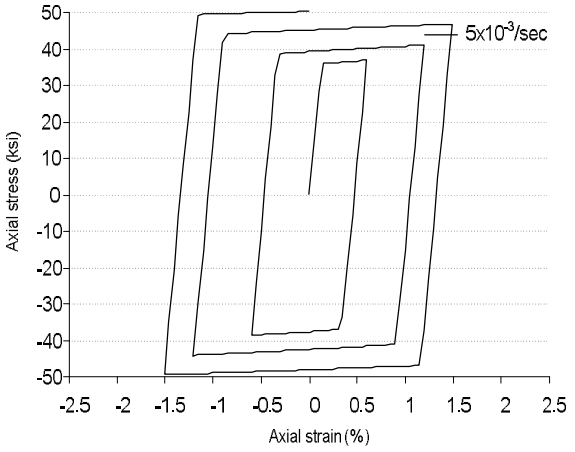

Fig. 13 Cyclic loading stress-strain response for strain rate of 5 x 10^{-3}/sec by rate dependent kinematic hardening model

6. Conclusions

In this paper, a rate dependent kinematic hardening model was used to understand inelastic behavior of metals subjected to monotonic loading. Two different types of cyclic loadings were considered and the numerical solutions are finally compared with experimental results. The numerical results obtained by the rate dependent kinematic hardening model does not give a good shape for the hysteresis loop. However, this model has good features, including a small number of parameters and a simple numerical algorithm. Thus, this model can be used for approximate and fast analysis of metals.

References

Abdel-Karim, M. and N. Ohno. (2000). "Kinematic Hardening Model Suitable for Ratchetting with Steady-State." *Int. J. Plast.,* Vol. 16, pp. 225-240.

Bodner, S. R. and Partom, Y. (1972). "A Large Deformation Elastic-viscoplastic Analysis of a Thick-walled Spherical Shell." *ASME, J. Appl. Mech.,* Vol. 39, pp. 751-757.

Chaboche, J. L. (1977). "Viscoplastic Constitutive Equations for the Description of Cyclic and Anisotropic Behavior of Metals." *Bull. Acad. Polon. Sci. Ser. Sci. Tech.,* Vol. 25. pp. 33-42.

Chaboche. J. L., Rousselier. (1983). "On the Plastic and Viscoplastic Constitutive Equations-Part I: Rule Developed with Internal Variable Concept." *Journal of Pressure Vessel Technology*, Vol. 105, No. 2, pp. 153-158.

Chaboche. J. L. (1989). "Constitutive Equations for Cyclic Plasticity and Cyclic Viscoplasticity." *IInt. J. Plast.,* Vol. 5, pp. 247-302.

Chang, K. C. and Lee, G. C. (1987). "Strain Rate Effect on Structural Steel Under Cyclic Loading." *J. Engrg. Mech, ASCE,* Vol. 113, No. 9, pp. 1292-1301.

Dunne, F. and Petrinic, N. (2005). Introduction to Computational Plasticity, Oxford, University Press.

Ellyin, F. and Xia, Z. (1991). "A Rate-Dependent Inelastic Constitutive Model, Part I: Elastic-Plastic Flow." *J. Engng. Mater. Technol. Trans., ASME,* Vol. 113, pp. 314-323.

Hart, E. W. (1976). "Constitutive Relations for the Nonelastic Deformation of Metals." *ASME, J. Eng. Mat. Tech,* Vol. 98, pp. 193-201.

Hibbit, Karlsson and Sorensen, Inc., (2008). Abaqus user's guide, v. 6.8. HKS Inc. Pawtucket, RI, USA.

Kang, G. Z. and Gao, Q. (2004). "Temperature-dependent cyclic deformation of SS304 stainless steel under non-proportionally multi axial load and its constitutive modeling." *Key Eng. Mater.* Vol. 275–276, pp. 247–252.

Kang, G. Z., Kan, Q. H., and Zhang, J. (2006). "Time - dependent ratcheting experiments of SS304 stainless steel." *Int. J. Plast.,* Vol. 22, pp. 858–894.

Krempl, E. (1979). "An Experimental Study of Room Temperature Rate Sensitivity, Creep and Relaxation of AISI Type 304 Stainless Steel." *J. Mech. Phys. Solids.,* Vol. 27. pp. 363.

Lemaitre, J. (2001). Handbook of Materials Behavior Models. Academic Press.

McDowell, D. L. (1992). "A Nonliear Kinematic Hardening Theory for Cyclic Thermoplasticity and Thermoviscoplasticity." *Int. J. Plast.,* Vol. 8, pp. 695-728.

Miller, A. (1976). "An Inelastic Consitutive Model for Monotonic, Cyclic, and Creep Deformation." *ASME, J. Eng. Mat. Tech,* Vol. 98, pp. 97-113.

Ohno, N. and Wang, J. D. (1993). "Kinematic Hardening Rules with Critical State for Activation of Dynamic Recovery, Part I, Formulation and Basic Features for Ratchetting Behavior." *Int. J. Plast.*, Vol. 9, pp. 375-390.

Ramaswamy, V. G., Stouffer, D. C., and Laflen, J. H. (1990). "A Unified Constitutive Model for the Inelastic Uniaxial Response of Rene 80 at Temperatures Between 538C and 982C." *J. Eng. Mat. Tech,* 112.

Robinson, D. N., Pugh, C. E., and Corum, J. M. (1976) "Constitutive Equations for Describing High - temperature Inelastic Behavior of Structural Alloys, in Specialists Meeting on High - temperature Structural Design Technology of LMFBRs, IAEA report IWGFR/11." *International Atomic Energy Agency,* pp. 44-57.

Tanaka, E. and Yamada, H. (1993). "Cyclic creep, mechanical ratchetting and amplitude history dependence of modified 9Cr–1Mo steel and evaluation of unified constitutive models." *Trans. JSME(A),* Vol. 59, pp. 2837–2843.

Tanaka, E. (1994). "A non-proportionality Parameter and a Viscoplastic Constitutive Model Taking into Amplitude Dependences and Memory Effects of Isotropic Hardening." *Eur. J. Mech. A/Solids,* 13.

Yaguchi, M. and Takahashi, Y. (2000). "A viscoplastic constitutive model incorporating dynamic strain aging effect during cyclic deformation conditions." *Int. J. Plast.,* Vol. 16, pp. 241–262.

Yaguchi, M. and Takahashi, Y. (2005). "Ratchetting of viscoplastic material with cyclic softening. Part 2. Application of constitutive models." *Int. J. Plast.,* Vol. 21, pp. 835–860.